

ChemSusChem

Supporting Information

Influence of Vacancies in Manganese Hexacyanoferrate Cathode for Organic Na-Ion Batteries: A Structural Perspective

Min Li, Mattia Gaboardi, Angelo Mullaliu, Mariam Maisuradze, Xilai Xue, Giuliana Aquilanti, Jasper Rikkert Plaisier, Stefano Passerini,* and Marco Giorgetti*This publication is part of a joint Special Collection of ChemSusChem, Batteries & Supercaps, and Energy Technology including invited contributions focusing on the “International Conference on Sodium Batteries (ICNaB)”. Please visit [to view all contributions.](#) © 2023 The Authors. ChemSusChem published by Wiley-VCH GmbH. This is an open access article under the terms of the Creative Commons Attribution License, which permits use, distribution and reproduction in any medium, provided the original work is properly cited.

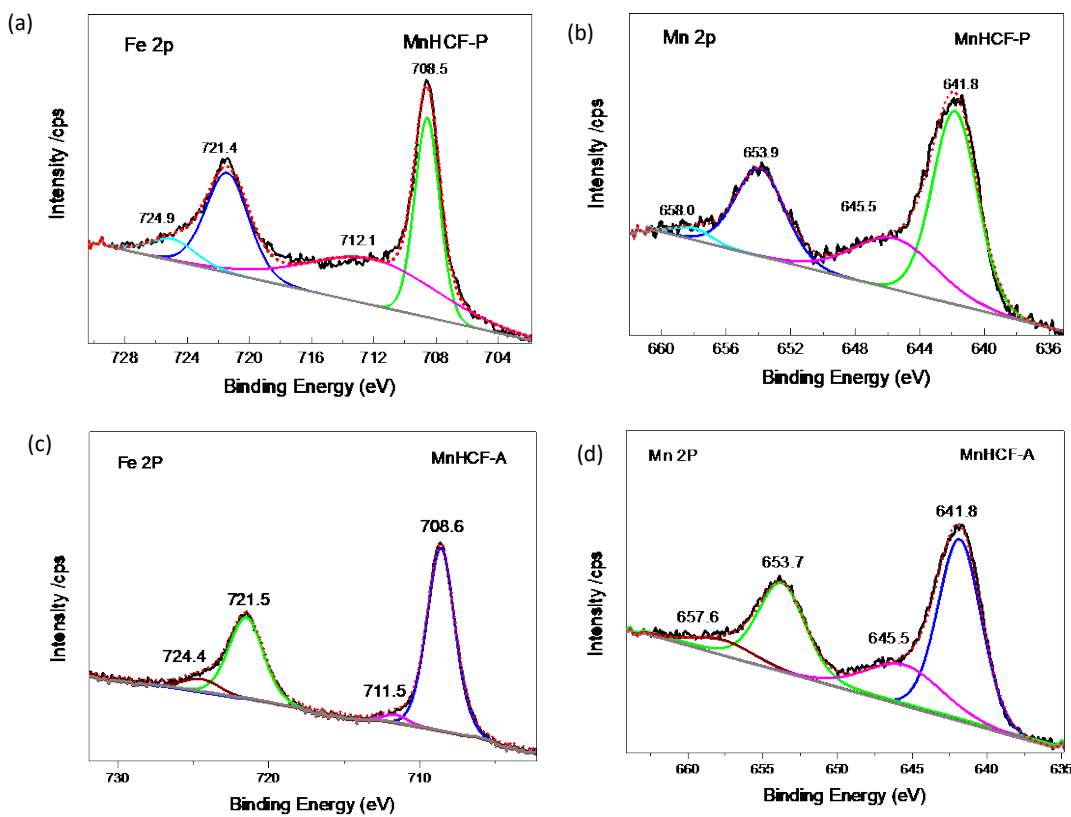


Figure S1 Fe 2P and Mn 2P XPS of MnHCF-P and MnHCF-A.

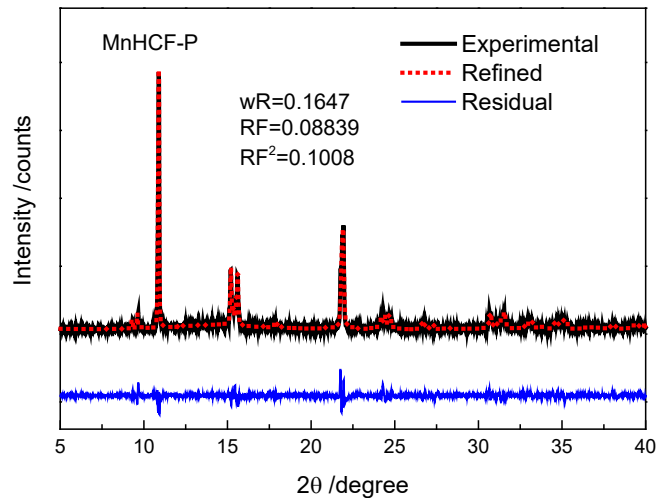


Figure S2. Rietveld refinement of MnHCF-P.

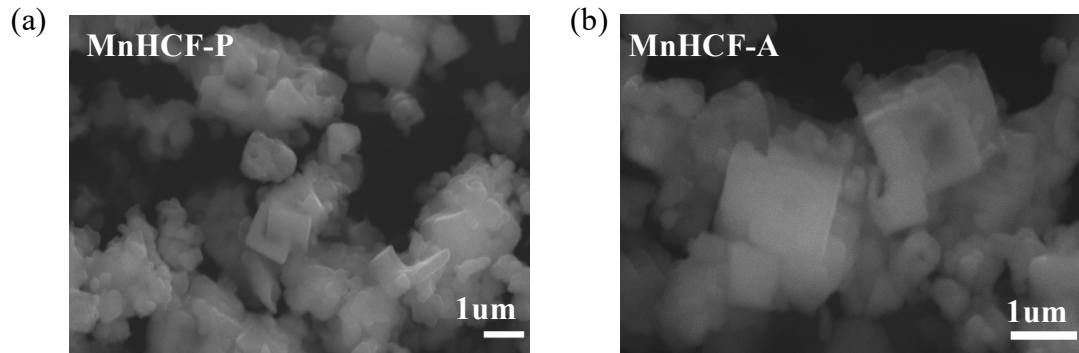


Figure S3 SEM image of (a) MnHCF-P and (b) MnHCF-A.

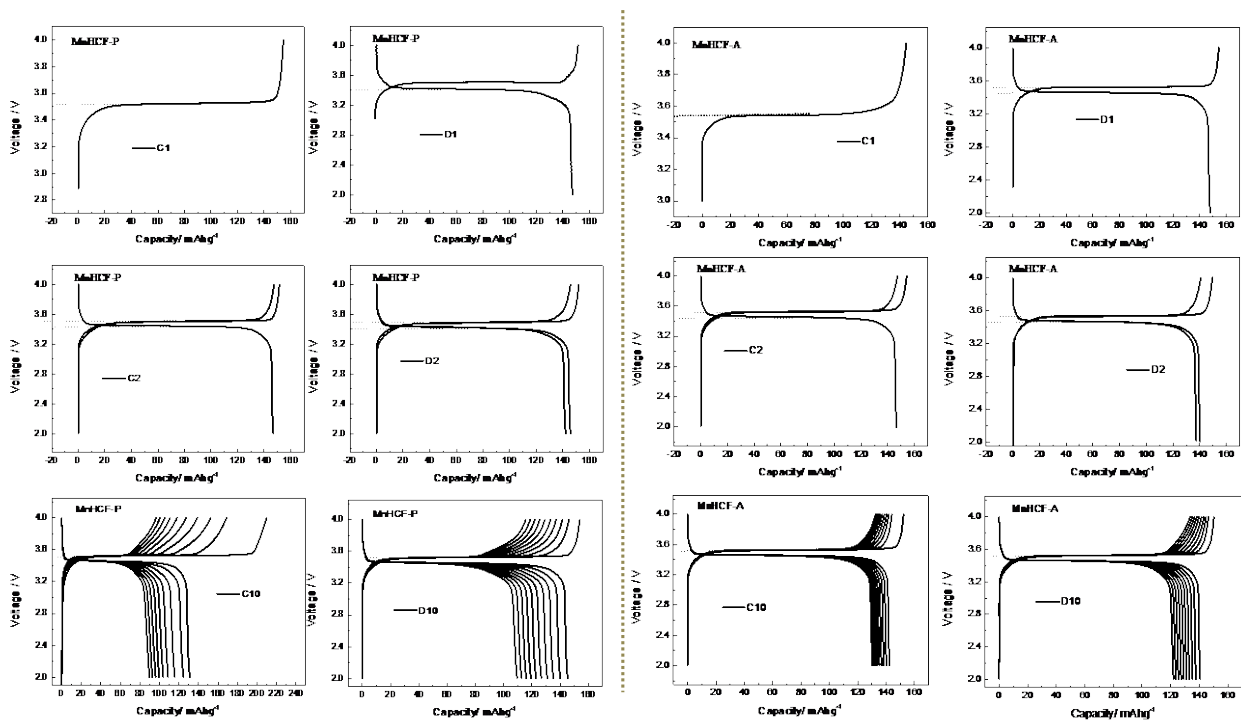


Figure S4. Galvanostatic charge/discharge curves recorded for all MnHCF-P/A ex-situ electrodes.

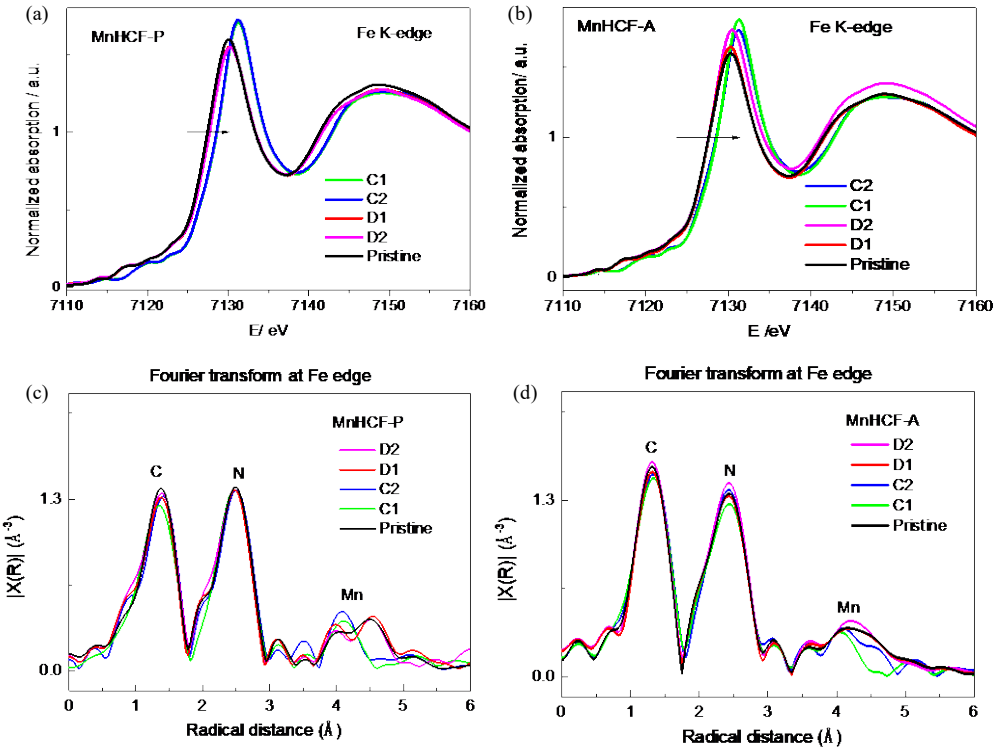


Figure S5 (a, b) Ex-situ XANES spectra of Fe K-edge for MnHCF-P/A samples; (c, d) Corresponding Fourier transforms of k^2 -weighted EXAFS signals at Fe- K-edge.

EXAFS Analysis

The Extended X-ray Absorption Fine Structure (EXAFS) analysis was performed using the GNXAS package [si1, si2] which is based on the Multiple Scattering (MS) theory. The method uses the decomposition of the EXAFS signals into a sum of several contributions, namely the n-body terms. The theoretical signal is calculated ab-initio and contains the relevant two-body $\gamma(2)$, three-body $\gamma(3)$, and four-body $\gamma(4)$ MS terms [si3]. The two-body terms are associated with pairs of atoms and probe their distances and variances. The three-body terms are associated with triplets of atoms and probe angles, and bond-bond and bond-angle correlations. The four-body terms are associated to chains of four atoms, and probe distances and angles in-between, and bond-bond and bond-angle correlations. However, since Fe-C-N-Mn chains feature angles in-between close to 180° , the actual number of parameters used to define the $\gamma(3)$ or the $\gamma(4)$ peaks was reduced by symmetry. More details on the use of parameters correlation in the four-body term is out of the aim of the present work and can be found in the references [si4, si5]. Data analysis was performed by minimizing a χ^2 -like residual function that compares the theoretical (model) signal, $\mu_{\text{mod}}(E)$, to the experimental one, $\mu_{\text{exp}}(E)$. The phase shifts for the photoabsorber and backscatterer atoms were calculated starting from the structure reported by Song et al. [si6] according to the muffin-tin approximation and allowing 10% overlap between the muffin-tin spheres. The Hedin-Lundqvist complex potential [si7] was used for the exchange-correlation

potential of the excited state. The core-hole lifetime, Γ_c , was fixed to the tabulated value [si8] and was included in the phase shift calculation.

Table S1. EXAFS fitting parameters. Errors in parenthesis have been obtained by two dimensional section of the parameter space (contour plots), selected among the parameters having strong correlation.

	Pristine MnHCF- P	C1	D1	C2	D2	Pristine MnHCF -A	C1	D1	C2	D2
Fe-C / Å	1.877(5)	1.900(2)	1.877(6)	1.896(6)	1.876(4)	1.878(6)	1.902(4)	1.870(6)	1.900(4)	1.878(4)
σ^2 Fe-C / Å ²	0.003(1)	0.003(1)	0.003(1)	0.003(1)	0.003(1)	0.003(1)	0.003(1)	0.003(1)	0.003(1)	0.003(1)
C≡N / Å	1.187(4)	1.162(3)	1.178(6)	1.160(5)	1.178(5)	1.188(5)	1.161(6)	1.18(1)	1.16(1)	1.18(1)
σ^2 C≡N / Å ²	0.008(3)	0.006(3)	0.006(3)	0.007(3)	0.012(3)	0.008(3)	0.009(2)	0.005(2)	0.011(2)	0.007(2)
Mn-N / Å	2.183(1) ^a	1.95(1) ^b	2.18(1) ^a	2.00(1) ^b	2.183(1) ^a	2.191(1) ^a	1.962(7) ^b	2.12(1) ^b	1.96(2) ^b	2.14(2) ^b
σ^2 Mn-N / Å ²	0.007(2)	0.006(2)	0.006(2)	0.009(3)	0.007(2)	0.005(3)	0.009(2)	0.005(2)	0.005(2)	0.010(2)
Mn-N / Å		2.21(1) ^c		2.26(2) ^c			2.18(2) ^c	2.19(1) ^c	2.21(3) ^c	2.19(3) ^c
σ^2 Mn-N / Å ²		0.013(6)		0.004(2)			0.004(2)	0.007(3)	0.018(8)	0.005(2)
θ Fe-C-N / deg	175 FIX	175 FIX	175 FIX	175 FIX	175 FIX	175 FIX	175 FIX	175 FIX	175 FIX	175 FIX
θ Mn-N-C / deg	175 FIX	175 FIX	175 FIX	175 FIX	175 FIX	175 FIX	175 FIX	175 FIX	175 FIX	175 FIX
E0 Mn	6542(1)	6542(1)	6542(1)	6546(1)	6544(1)	6542(1)	6541(1)	6540(1)	6543(2)	6541(1)
E0 Fe	7118(1)	7119(1)	7118(1)	7118(1)	7118(1)	7118(1)	7118(1)	7117(1)	7118(1)	7117(1)
S02 Mn	0.68(3)	0.68 FIX	0.68 FIX	0.68 FIX	0.68 FIX	0.68 FIX	0.68 FIX	0.68 FIX	0.68 FIX	0.68 FIX
S02 Fe	0.81(5)	0.81 FIX	0.81 FIX	0.81 FIX	0.81 FIX	0.81 FIX	0.81 FIX	0.81 FIX	0.81 FIX	0.81 FIX
χ^2 -like residual / (10^{-6})	2.24	3.46	5.36	3.62	2.65	2.17	2.42	4.11	1.88	3.23

^aCN =6. ^bCN=4. ^cCN=2

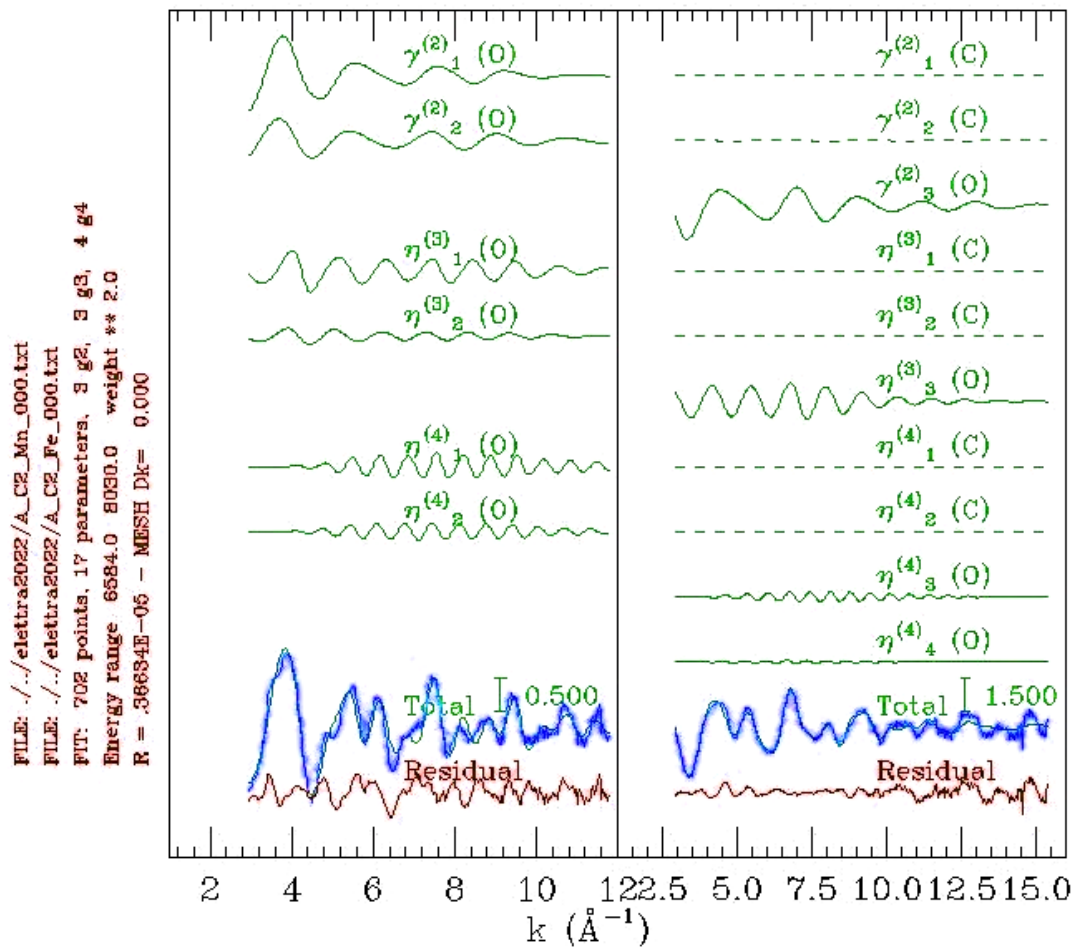


Figure S6. Details of the EXAFS two-edges analysis (Mn and Fe) of MnHCF-A C2, in terms of single terms contribution to the total overall EXAFS signals.

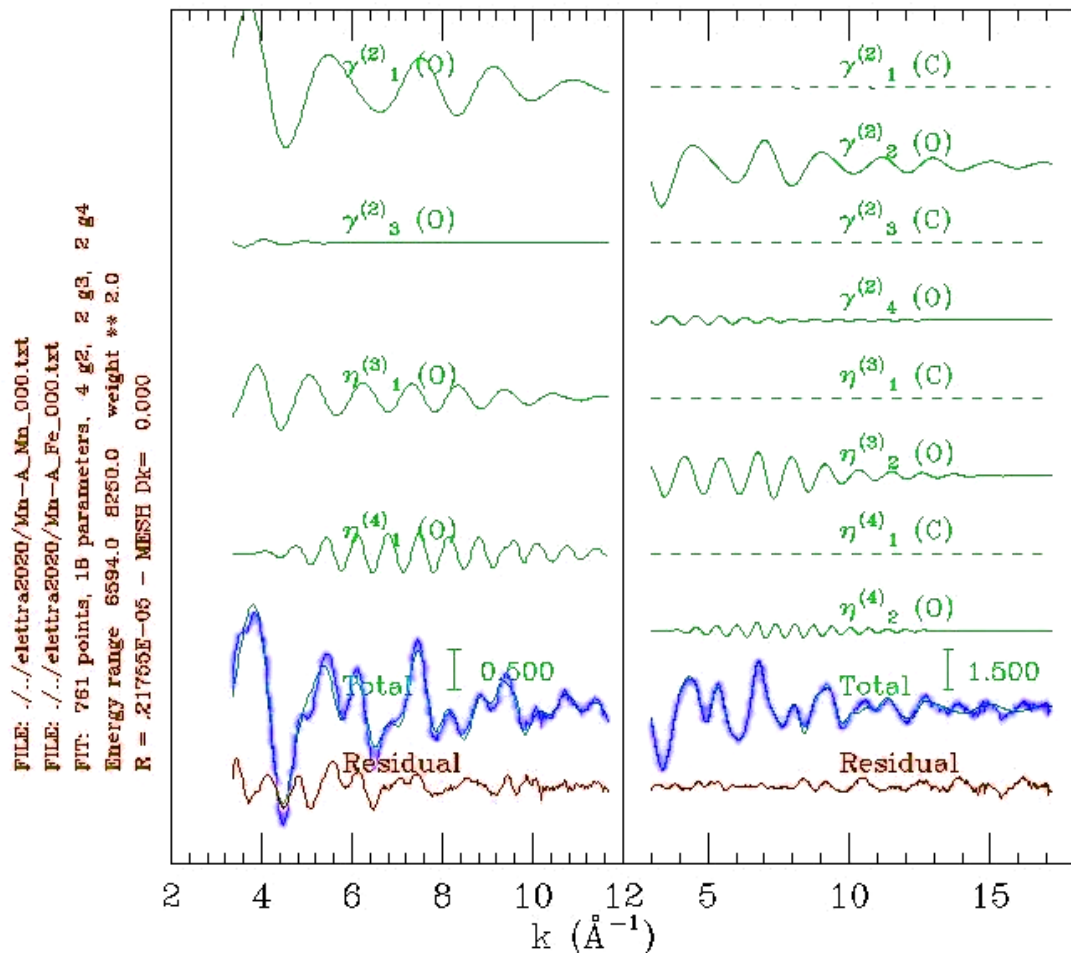


Figure S7. Details of the EXAFS two-edges analysis (Mn and Fe) of pristine MnHCF-A, in terms of single terms contribution to the total overall EXAFS signals.

- [si1] A. Filippioni, A. Di Cicco, C.R. Natoli, X-ray-absorption spectroscopy and n-body distribution functions in condensed matter. I. Theory, Phys. Rev. B. 52 (1995) 15122–15134. doi:10.1103/PhysRevB.52.15122
- [si2] A. Filippioni, A. Di Cicco, X-ray-absorption spectroscopy and n -body distribution functions in condensed matter. II. Data analysis and applications, Phys. Rev. B. 52 (1995) 15135–15149. doi:10.1103/PhysRevB.52.15135.
- [si3] M. Giorgetti, M. Berrettoni, A. Filippioni, P.J. Kulesza, R. Marassi, Evidence of four-body contributions in the EXAFS spectrum of Na₂Co[Fe(CN)₆], Chem. Phys. Lett. 275 (1997) 108–112. doi:10.1016/S0009-2614(97)00724-0.
- [si4] M. Giorgetti, M. Berrettoni, Structure of Fe/Co/Ni hexacyanoferrate as probed by multiple edge X-ray absorption spectroscopy, Inorg. Chem. 47 (2008) 6001–6008. doi:10.1021/ic800289c.
- [si5] M. Giorgetti, L. Guadagnini, D. Tonelli, M. Minicucci, G. Aquilanti, Structural characterization of

electrodeposited copper hexacyanoferrate films by using a spectroscopic multi-technique approach, Phys. Chem. Chem. Phys. 14 (2012) 5527–5537. doi:10.1039/c2cp24109a.

[si6] J. Song, L. Wang, Y. Lu, J. Liu, B. Guo, P. Xiao, J.J. Lee, X.Q. Yang, G. Henkelman, J.B. Goodenough, Removal of interstitial H<inf>2</inf>O in hexacyanometallates for a superior cathode of a sodium-ion battery, J. Am. Chem. Soc. 137 (2015) 2658–2664. doi:10.1021/ja512383b.

[si7] L. Hedin, B. I. Lundqvist, S. Lundqvist, Local exchange-correlation potentials, Solid State Commun. 9 (1971) 537–541. doi:10.1016/0038-1098(71)90141-4.

[si8] M.O. Krause, J.H. Oliver, Natural widths of atomic K and L levels, K α X-ray lines and several K L L Auger lines, J. Phys. Chem. Ref. Data. 8 (1979) 329–338. doi:10.1063/1.555595.

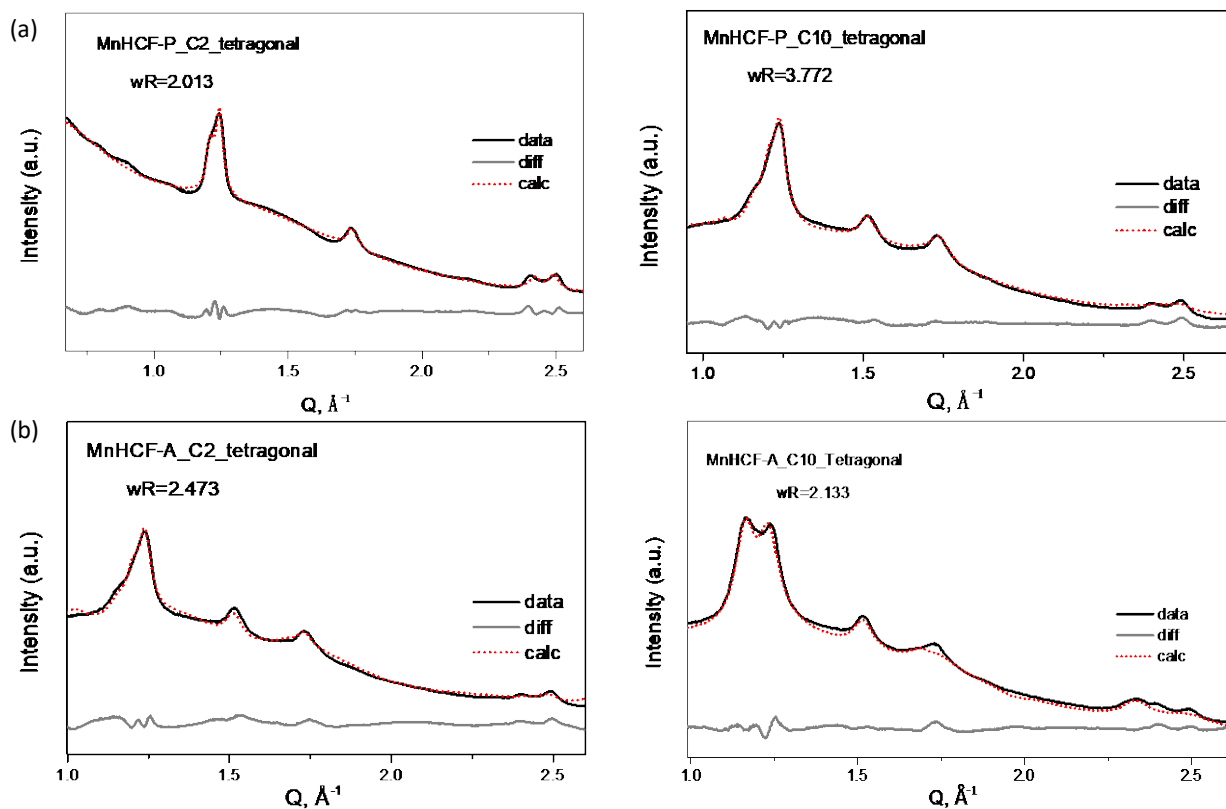


Figure S8. Pawley refinement results of C2, C10 charged electrodes of MnHCF-P and MnHCF-A based on tetragonal phase.

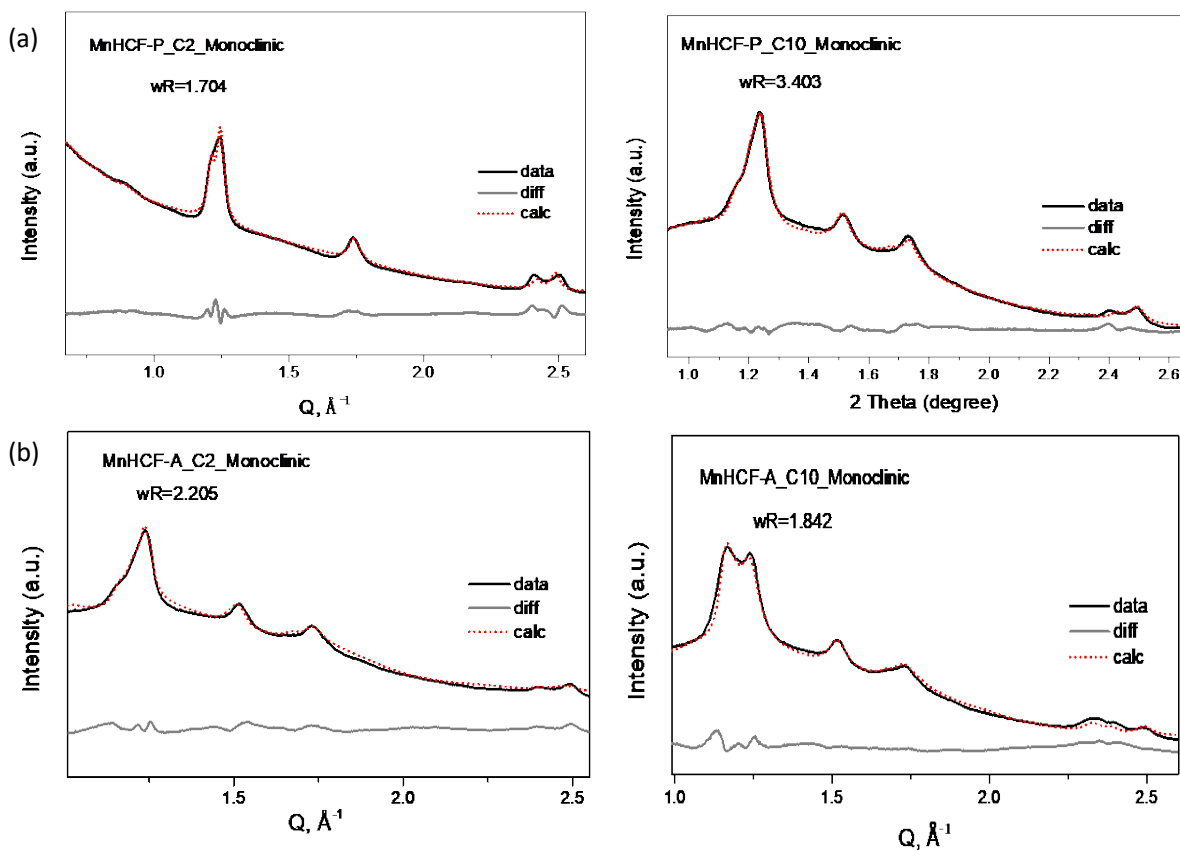


Figure S9. Pawley refinement results of C2, C10 charged electrodes of MnHCF-P and MnHCF-A based on monoclinic phase.

Table S2 refine result from tetragonal phase.

MnHCF-P	a(Å)	b(Å)	c(Å)	$\beta(^{\circ})$	Vol(Å ³)
P-electrode	10.46263(28)	7.547(27)	7.230(27)	91.619(19)	570.727(3)
C1	7.128(5)	7.128(5)	10.375(4)	90	527.177(9)
D1	10.538(25)	7.502(28)	7.297(27)	91.453(21)	576.747(28)
C2	7.1548(23)	7.154(23)	10.409(6)	90	532.89(4)
D2	10.550(5)	7.508(4)	7.311(4)	91.781(4)	578.891(27)
C10	7.153(26)	7.153(26)	10.413(22)	90	534(5)
D10	10.521(6)	7.567(4)	7.303(5)	91.862(4)	581.165(13)
MnHCF-A	a(Å)	b(Å)	c(Å)	$\beta(^{\circ})$	Vol(Å ³)
P-electrode	10.478(5)	7.518(4)	7.204 (3)	91.316 (25)	567.7(7)
C1	7.1491(14)	7.1491(14)	10.458(9)	90	534.9(26)
D1	10.54 (27)	7.539(21)	7.253(24)	91.956(2)	576.08(4)
C2	7.1453(6)	7.14536)	10.497(9)	90	535.933(4)
D2	10.522(9)	7.478(5)	7.284(6)	91.589(7)	573.018(11)
C10	7.14(1)	7.14(1)	10.5(13)	90	541.868(17)
D10	10.541(9)	7.48(17)	7.34(9)	91.895(1)	579.108(15)

Table S3 refine result from monoclinic phase.

MnHCF-P	a(Å)	b(Å)	c(Å)	$\beta(^{\circ})$	Vol(Å ³)
P-electrode	10.4351(28)	7.4402(27)	7.3825(27)	92.492(19)	572.6(3)
C1	10.3817 (4)	7.086(5)	7.167(5)	90.52(10)	527.2(4)
D1	10.4454 (25)	7.5322(28)	7.250(27)	91.493(21)	573.64(28)
C2	10.4109 (30)	7.208(5)	7.126(5)	90.6(14)	531.46(28)
D2	10.4451 (5)	7.438(4)	7.355(4)	92.1(4)	574.37(27)
C10	10.357(15)	7.215(14)	7.035(17)	90.70(21)	525.6(18)
D10	10.490(6)	7.43(4)	7.38(5)	91.2(4)	575.0(13)
MnHCF-A	a(Å)	b(Å)	c(Å)	$\beta(^{\circ})$	Vol(Å ³)
P-electrode	10.4541(28)	7.5328(25)	7.2206(23)	91.663(16)	568.38(26)
C1	10.431(15)	7.169(19)	7.103(20)	90.96(22)	531.1(18)
D1	10.505(8)	7.554(8)	7.238(8)	91.62(6)	574.2(9)
C2	10.364(8)	7.063(6)	7.1692(4)	90.91(8)	524.81(5)
D2	10.486(5)	7.529(5)	7.225(5)	91.6(4)	570.1(6)
C10	10.5327(7)	7.0413(5)	7.1851(9)	90.84(4)	532.8(32)
D10	10.542(9)	7.6642(8)	7.2162(6)	91.5(12)	582.9(9)